

Table 2. Dissolved oxygen and hydrogen sulfide in Pingo Lake, Alaska on 23 July 1965.

Depth (m)	O <sub>2</sub> (ppm)	H <sub>2</sub> S (ppm)
0	11.1	
2	1.7	0
3	0	0
4	0	>5
6	0	>10
8		>20

Table 3. Concentration (mg/liter) of various substances in spring and well water near Pingo Lake, Alaska.

Ion	Arctic Circle Hot Springs	Circle City well water
Ca	29*	18.9
Mg	2.1*	0.3
K	8.6*	10.8
Na	248*	260
HCO <sub>3</sub>	173*	190
Cl	252*	246
So <sub>4</sub>	98*	
H <sub>2</sub> S		2-5
		0
	<i>Total dissolved solids</i>	
	816*	878
		277

\* Values posted at Arctic Circle Hot Springs by John Berdahl.

highest values recorded for lake water (6, 8). The fact that lithium is a common constituent in the water of mineral springs (6) supports the suggestion that the meromixis in Pingo Lake is maintained by crenogenic factors. The discrepancy in calcium content between 1964 and 1965 is thought to have been the result of biological activity or faulty analysis in 1964. Mostly constant values for the other ions, particularly below 3 m, were observed on all three dates.

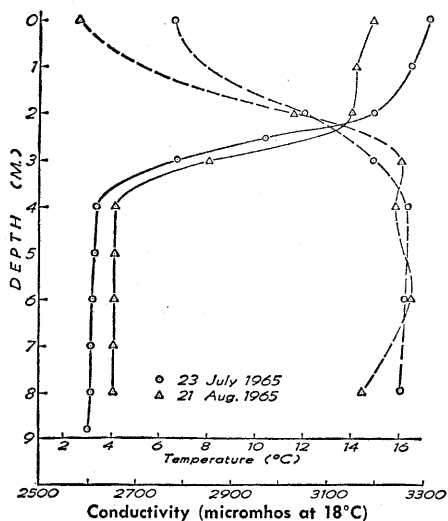


Fig. 3. Temperature (—) and conductivity (---) profiles in Pingo Lake.

One of the most common features of meromixis is an absence of dissolved oxygen and the presence of hydrogen sulfide in the deep waters (1). Such a condition is well developed in Pingo Lake (Table 2). Although this environment may be highly toxic to organisms, specialized biological communities may develop. For example, the larvae of the midge, *Chaoborus* sp., were found in abundance in Pingo Lake and might be expected to inhabit the deeper zones (9). Anaerobic bacteria also are common components of this community.

It is interesting to compare the chemical compositions of Pingo Lake with well water at Circle City (20 km northeast), and spring water at Arctic Circle Hot Springs (25 km south). Some of the more important chemical constituents are given in Table 3. On the basis of the ions found to be most abundant, the water in Pingo Lake can be classified as a sodium sulfate type, whereas that of Arctic Circle Hot Springs is predominately a sodium chloride type, and well water from Circle City is a calcium carbonate type.

Pingo Lake differs markedly from nearby lakes; the basin is deeper and the water contains more dissolved solids. The discovery of permanent chemical stratification and the associated biological zonation now provides an opportunity to study these phenomena in a subarctic environment (10).

G. E. LIKENS

Department of Biological Sciences,  
Dartmouth College, Hanover,  
New Hampshire

P. L. JOHNSON

U.S. Army Cold Regions Research and  
Engineering Laboratory, Hanover

#### References and Notes

1. G. E. Likens, in *Symposium on Meromictic Lakes* (Syracuse Univ. Press, Syracuse, N.Y.), in press.
2. D. B. Krinsley, *U.S. Geol. Surv. Profess. Papers No. 525-C*, p. 133 (1965).
3. F. Müller, *Meddelelser om Grønland* 183, No. 3, 127 pp. (1959).
4. G. W. Holmes, D. M. Hopkins, H. L. Foster, in *Proceedings International Conference on Permafrost*, Purdue University, R. W. Spangler, Ed. (National Academy of Sciences-National Research Council, Washington, D.C., 1960).
5. A. Long, *Radiocarbon* 7, 245 (1965).
6. G. E. Hutchinson, *A Treatise on Limnology* (Wiley, New York, 1957).
7. Anonymous, *U.S. Army Cold Reg. Res. Eng. Lab. Tech. Rep. No. 100* (1962).
8. D. A. Livingstone, *U.S. Geol. Surv. Profess. Papers No. 440-G* (1963).
9. D. G. Frey, *Mem. Ist. Ital. Idrobiol. suppl.* 8, 141 (1955).
10. Supported by U.S. Army Cold Regions Research and Engineering Laboratory (grants DA-AMC-27-021-69-09 and DA-AMC-27-021-65-G10). We thank T. Vogel, P. Fikkan, and M. Bailey for assistance.

23 May 1966

## Electrolytic Dissolution of Iron Meteorites

Abstract. When iron meteorites are dissolved anodically in neutral solution, nonmetallic inclusions are not attached and collect at the bottom of the anode compartment. When the meteorites contain both kamacite and taenite, the kamacite dissolves preferentially, revealing a three-dimensional Widmanstätten pattern.

The true chemical composition of nonmetallic inclusions in iron meteorites is difficult to establish with certainty by the usual chemical techniques. Many nonmetallic substances common to iron meteorites are completely destroyed or largely altered by acid attack during the dissolution process.

Metallic meteorites are composed primarily of iron-nickel alloys containing small amounts of cobalt, phosphorus, sulfur, and carbon. Meteorites with less than 6 percent nickel (by weight) contain a single metallic phase: kamacite. If the nickel content lies between 6 and 27 percent two metallic phases usually result: kamacite, containing 5.5 percent nickel (alpha phase), and taenite, containing 27 to 65 percent nickel (gamma phase). Meteorites containing more than 27 percent nickel have only the single-phase taenite. The orientation of the thick bands of kamacite and thin plates of taenite parallel with octahedral planes results in the familiar Widmanstätten structure (1).

Common nonmetallic inclusions in iron meteorites are schreibersite [(Fe,Ni)<sub>3</sub>P], troilite (FeS), daubreelite (FeCr<sub>2</sub>S<sub>4</sub>), cohenite (Fe<sub>3</sub>C), graphite (C), and sometimes the silicate minerals enstatite [(Mg,Fe)SiO<sub>3</sub>] and olivine [(Mg,Fe)<sub>2</sub>SiO<sub>4</sub>] (2).

Inclusions in steel, especially carbides, have been successfully extracted by an electrolytic technique (3); the steel sample was made the anode and dissolved electrolytically in an electrolyte such as 5-percent citrate solution adjusted to pH 5.0 to eliminate acid attack; nonmetallic inclusions fell to the bottom of the anode compartment and were collected by filtration. Electrolytic dissolution of iron meteorites containing both kamacite and taenite phases results in preferential attack on the kamacite, revealing a three-dimensional Widmanstätten pattern as well as separating the nonmetallic inclusions.

We now describe electrolytic dissolution of iron meteorites and separa-

tion of their nonmetallic portions. The dissolution proceeds as expected, the kamacite being attacked first in preference to the taenite. Chemical attack by acids follows the same order and results in the visible Widmanstätten pattern, as does the natural weathering process.

Iron meteorites exposed to air and

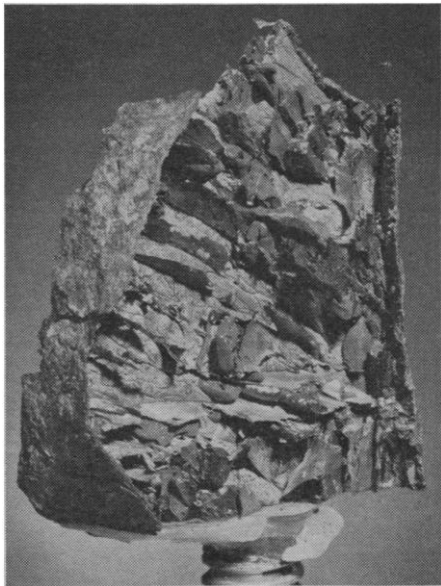


Fig. 1. Canyon Diablo meteorite after 20-hour electrolysis at 0.5 amp. The oxide coat was not removed from the edge of the specimen before electrolysis; diameter of the rod is 0.6 cm.

moisture are naturally weathered; corrosion occurs through local electrochemical cells according to the well-established principles of corrosion theory; the process in meteorites has been reviewed by Buddhue (4). Requirements for natural chemical corrosion include only (i) two sites of differing potential, (ii) an electrolyte solution connecting both sites, and (iii) electric conduction between the sites.

The most destructive combination for iron meteorites is the kamacite-taenite couple (4). Standard potentials for the  $Fe^{++}/Fe$  and  $Ni^{++}/Ni$  couples are  $-0.44$  and  $-0.24$  volt, respectively. In the simple kamacite-taenite couple, the more resistant taenite acts as the cathode while kamacite is the anode in a corrosion cell; the result is protection of the taenite and dissolution of the kamacite.

Many meteorite finds show invasive oxidation ranging from the initial to final stages; almost always the original Widmanstätten pattern is revealed (4).

When the entire sample of meteorite is made the anode in an electrolytic cell, iron is dissolved preferentially because of its favorable potential. The high nickel content of taenite preserves its structure; preservation is further enhanced by the existence of nickel-rich borders in the taenite phase—microprobe analyses show that the nickel

content of taenite is much higher at the taenite-kamacite interfaces (5). The oxidized iron ( $Fe^{++}$ ) is soluble in the electrolyte solution, and the kamacite dissolves readily; much of its nickel is left as a metallic sludge at the bottom of the anode compartment. The overall electrolysis reveals a three-dimensional Widmanstätten pattern in meteorites containing both kamacite and taenite. As the metal dissolves, nonmetallic inclusions and separated taenite flakes fall to the bottom of the anode compartment. Near the end of the kamacite dissolution, the remnant sample consists of thin metallic taenite lamellae extending outward from the undissolved kamacite core (Figs. 1-4).

Our apparatus resembles that of Gurry *et al.* (3). The electrolytic cell is contained in an inverted sawn-off 2-liter bottle. Anode and cathode compartments are concentric, the inner anode compartment being separated from the cathode section by cellophane dialysis tubing which permits electrical contact without mixture of solutions. A sheet of copper foil lining the container serves as cathode. The meteorite sample is supported by a stainless steel rod, at the top of which is mounted a vibrator to shake isolated particles from the sample. Both compartments are sealed with concentrically mounted neoprene stoppers. Gas inlet and exit tubes are fitted through the stoppers so that both anode and cathode compartments can be deaerated. In the bottom of the anode compartment are a large-bore stopcock and ball joint to facilitate removal of the anolyte and filtration of the residue. Electricity is supplied by a lead storage battery containing a 6-ohm 25-watt rheostat as a voltage divider. Reagent-grade chemicals are used throughout.

The meteorite samples, about 2 by 1 by 1 cm, were ground free of rust with a carborundum wheel. The largest flat surface was then polished to aid observation of structure during the initial stage of the dissolution process. The sample was attached to the stainless-steel rod in this manner: A hole  $3/16$  inch (4.8 mm) in diameter was drilled in one end of the sample to a depth of  $1/8$  to  $1/4$  inch, and the tapered end of the rod was forced into the hole. A drop of epoxy cement placed on the surface at the junction and allowed to cure prevented accidental dislodgment of the sample by the vibrator during electrolysis. Coating the support rod with molten beeswax prevented its con-

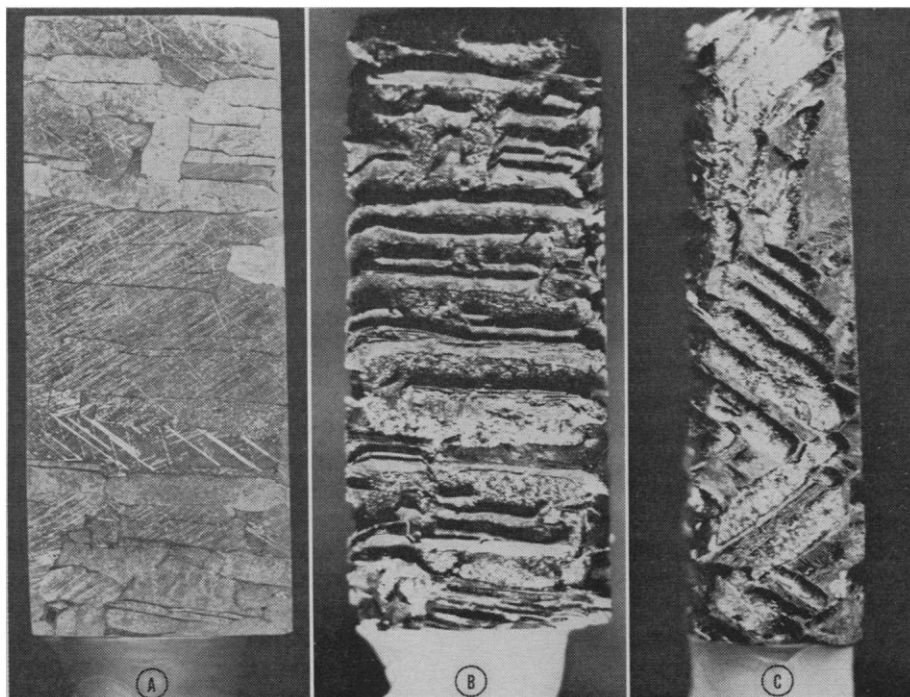


Fig. 2. The Xiquipilco sample at various stages. A, Etched but not electrolyzed (1.2 by 3 cm, front view); B, front view after 10-hour electrolysis; C, side view after 8-hour electrolysis; the oxide coating (upper right) was not removed; the side measures 3 by 0.6 cm.

tact with the electrolyte solution. The sample was finally cleaned by immersion in 1 : 1 HCl or 6-percent HNO<sub>3</sub> for about 2 minutes, rinsed thoroughly in water, rinsed with absolute alcohol, and dried.

The wet-dialysis tubing was stretched over the glass sleeves at the top and bottom of the anode compartment, the copper cathode was placed in the cell, and both compartments were filled with 0.5M cadmium iodide. Care was taken to fill both compartments simultaneously, since a difference in surface height would have caused either rupture or collapse of the dialysis tubing. The solutions were deaerated by bub-

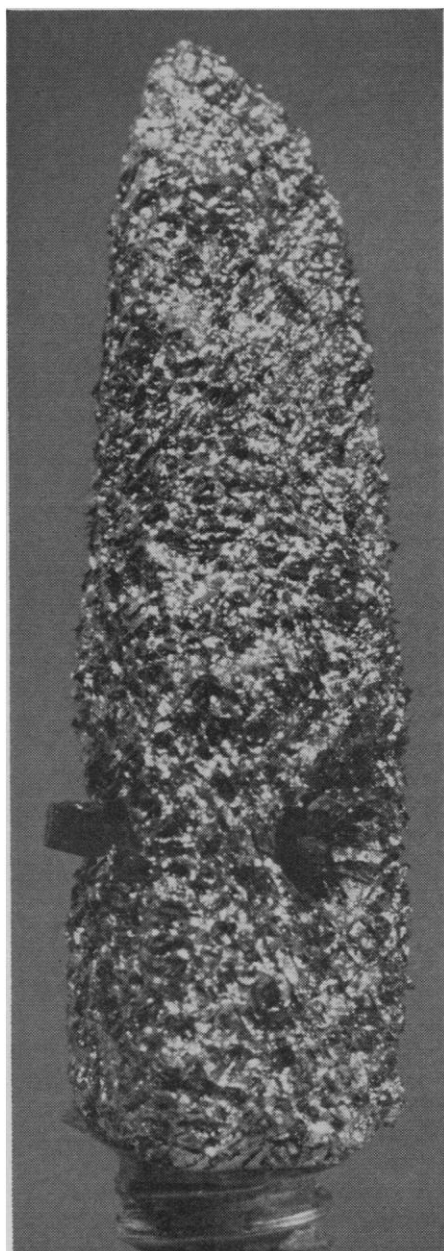


Fig. 3. The Santiago Papasquero meteorite, showing a schreibersite inclusion after 24-hour electrolysis; diameter of the rod is 0.6 cm.

bling purified nitrogen through them for 30 minutes, and nitrogen was passed over the surface throughout the electrolysis to prevent diffusion of oxygen into the cell.

The sample was placed just under the surface of the anode compartment, the vibrator was turned on, and the electrolysis started (negative lead to the copper sheet, positive lead to the rod holding the sample). The voltage was adjusted until the electrolysis current was about 0.5 amp; currents greater than 1 amp caused direct formation of ferric iron and precipitation of hydrous ferric oxide. Some of the electrolyses were interrupted periodically for photography of the samples; after each photograph the sample was returned to the cell and electrolysis was resumed.

When electrolysis was finally stopped, the remaining sample was removed, and the cathode was drained slowly, while the anolyte was drained directly through a sintered-glass crucible and collected in a filter flask. All residue was washed from the anode compartment into the filter crucible, washed thoroughly with water, rinsed with alcohol, and dried.

Under a microscope the particles of dried residue were separated visually according to shape, color, appearance, and so on. The nonmetallic residue was identified by its x-ray powder diffraction pattern obtained in the usual manner. Metallic particles that could not be ground to powder easily were identified by their x-ray fluorescence spectra.

The first meteorite sample (Canyon Diablo; coarse octahedrite) was electrolyzed without removal of the oxide coating from the weathered surface. While the kamacite dissolved readily, the taenite bands and ferric oxide surface remained intact (Fig. 1). Some of the fragile taenite sheets, dislodged from the sample, were collected with the other residue from the bottom of the anode compartment.

A specimen of the Xiquipilco, Mexico, meteorite, a medium octahedrite, measuring about 3 by 1.2 by 0.7 cm, was polished and photographed periodically during the dissolution process; Fig. 2 is a series of photographs before and during dissolution. (Electrolysis was stopped before all kamacite dissolved.)

A sample of the Santiago Papasquero, Mexico, meteorite, measuring 3 by 1 by 0.8 cm, was similarly treated. This meteorite has a nickel content of 7.50 percent (5) but does not exhibit



Fig. 4. Canyon Diablo meteorite after 15-hour electrolysis at 0.5 amp; diameter of the rod is 0.6 cm.

the expected octahedral Widmanstätten pattern; its relatively homogeneous structure may reflect obliteration of the original Widmanstätten structure by extensive reheating after the initial formation. In contrast with Canyon Diablo and Xiquipilco, Santiago Papasquero showed no immediately obvious macro structure upon dissolution; Fig. 3 shows it after 24-hour electrolysis, when it remained shiny, its entire surface being covered with small pits. Examination of the treated surface under magnification showed slight indication of possible relict Widmanstätten structure.

An inclusion in the Santiago Papasquero meteorite is evident in Fig. 3; most probably schreibersite, it is about 1 cm long, protrudes from both the front and rear faces, and has a roughly diamond-shaped cross-sectional area of about 1 by 2 mm. Interesting was the more rapid dissolution of the metal surrounding the inclusion: such inclusions are usually surrounded by kamacite, known as swathing kamacite, so that they are not in contact with taenite. This more rapid dissolution of the swathing kamacite is further evidence of a possible relict Widmanstätten structure.

Residues from electrolysis of the Canyon Diablo, Xiquipilco, and Santiago Papasquero meteorites all contained schreibersite, taenite, and kamacite; cohenite also occurred in the Canyon Diablo residue. Since the electrolysis is specific for the dissolution of metallic material, occurrence of kama-

cite and taenite in the residue reflects mechanical dislodgment by the vibrator during electrolysis. The absence of identifiable troilite from the residue is somewhat surprising, but the samples were fairly small and only a few millimeters of kamacite was dissolved; complete dissolution would no doubt leave troilite nodules.

At currents of 0.5 amp or less, only the iron appeared to stay in solution on dissolution of kamacite, while nickel ended up as a metallic sludge at the bottom of the anode compartment. More nickel dissolved when higher currents were applied, even though the standard potential of the nickelous-nickel couple ( $-0.24$  volt) is 0.2 volt more positive than the standard potential of the ferrous-iron couple ( $-0.44$  volt). At currents exceeding 1 amp, some ferric iron was formed. The standard potential of the ferric-ferrous couple is  $+0.773$  volt—considerably more positive than the nickelous-nickel couple. At low currents, however, the extent of nickel dissolution was slight and the taenite structure was maintained while kamacite dissolved entirely.

A Canyon Diablo specimen measuring about 2 by 2 by 0.8 cm was electrolyzed until about 35 g of metal was taken into solution; finally it appeared identical with the Canyon Diablo specimen in Fig. 4; analysis of the electrolyte solution showed that nickel comprised only 1.5 percent of the total dissolved metal. Since kamacite contains approximately 5.5 percent nickel, the remaining nickel must have either plated-out on the taenite lamellae or separated from the solution as metallic nickel. X-ray fluorescence analysis of the residue showed a high nickel content. Analysis of a sample of taenite that was carefully removed from the specimen gave 40.1 percent iron and 59.9 percent nickel, a composition within the normal range of taenite but somewhat richer than the 31 to 34 percent nickel reported for taenite in the Canyon Diablo meteorite (7). The nickel content found here for taenite was still too low to account for the remainder of nickel from the kamacite phase; thus it was concluded that the metallic nickel had indeed collected at the bottom of the anode compartment.

If metallic iron is brought into contact with a solution of a more noble metal, the other metal is reduced by the iron; it plates out onto the iron and an equivalent amount of iron dissolves.

Dissolution of the iron dislodges the noble metal which settles to the bottom of the container as a metallic sludge. This principle is used in copper mining; "tin" cans are added to vats of acidic copper solutions, and metallic copper is recovered. Nickel from the dissolved kamacite may have been deposited analogously.

Electrolytic oxidation of iron meteorites in a suitable electrolyte solution results in preferential dissolution of metallic iron. Nonmetallic inclusions and, for the most part, metallic nickel remain undissolved. The high nickel content of taenite, and especially the nickel-rich borders in the taenite phase, result in preservation of its structure, while the high iron content of kamacite results in its dissolution. The remaining specimen shows a network of taenite plates in octahedral arrangement, with the kamacite removed. Nonmetallic inclusions and any oxide coating were untouched by the dissolution process (Figs. 1-4).

The electrolytic process is an excellent and previously unavailable technique for chemically separating metallic and nonmetallic phases of meteorites and for preferentially dissolving only

the kamacite in octahedrites. Since iron dissolves first because of its favorable potential, a three-dimensional Widmanstätten pattern can be easily revealed as desired. The dissolution of iron is followed by dissolution of nickel, but all nonmetallic phases remain completely untouched.

STANFORD L. TACKETT\*

WALLACE M. MEYER, JR.

FRANK G. PANY

CARLETON B. MOORE

Department of Chemistry,  
Arizona State University,  
Tempe

#### References and Notes

1. J. I. Goldstein and R. E. Ogilvie, *Geochim. Cosmochim. Acta* **29**, 893 (1965).
  2. B. Mason, *Meteorites* (Wiley, New York, 1962), pp. 53-69.
  3. R. W. Gurry, J. Christakos, C. D. Stricker, *Trans. Amer. Soc. Metals* **50**, 105 (1958).
  4. J. D. Buddhue, *The Oxidation and Weathering of Meteorites* (Univ. of New Mexico Press, Albuquerque, 1957), pp. 30-43.
  5. J. M. Short and C. A. Andersen, *J. Geophys. Res.* **70**, 3745 (1965).
  6. Analysis by C. F. Lewis, Arizona State University.
  7. T. B. Massalski and F. R. Park, *J. Geophys. Res.* **67**, 2925 (1962).
  8. Aided by NSF undergraduate research participation program (W.M.M. and F.G.P.).
- \* Present address: Department of Chemistry, Indiana University of Pennsylvania, Indiana, Pennsylvania.

16 May 1966

## Source of Lead-210 and Polonium-210 in Tobacco

*Abstract. Test plants were grown within a chamber enriched with radon-222 in the atmosphere, in tobacco fields with different sources of phosphate-containing fertilizer, and in culture containing lead-210 in the nutrient solution. Harvested leaves were subjected to three curing conditions. The major portion of the lead-210 in the plant was probably absorbed through the roots. Airborne radon-222 and its daughters contributed much less to the plant's content of lead-210 and of polonium-210. The stage of leaf development and the methods used to cure the leaf affected the final amount of polonium-210 in tobacco leaf.*

Current interest in the presence of  $Po^{210}$  in tobacco and tobacco smoke (1, 2) and recent reports on the variation of the amount of  $Po^{210}$  in leaf tobacco produced in different parts of the world (3) led us to investigate the source of  $Pb^{210}$  and  $Po^{210}$  in tobacco. Of the nuclides in the uranium series with longer half-lives,  $U^{238}$ ,  $Ra^{226}$ ,  $Pb^{210}$ , and  $Po^{210}$  are principally present in soil and fertilizer, while  $Rn^{222}$ , a chemically inert gas, and some of its short-lived daughter products, are present in the air. To determine whether any one of these nuclides is a possible source of  $Po^{210}$  in tobacco, the following experiments were conducted: (i) tobacco plants were grown in an atmosphere enriched with  $Rn^{222}$ , (ii) tobacco plants grown in the field and supplied

with regular commercial fertilizer containing superphosphate were compared with those supplied with specially mixed fertilizer containing chemically pure, secondary calcium phosphate; and (iii) tobacco was grown in a nutrient solution containing  $Pb^{210}$  as lead nitrate in equilibrium with  $Po^{210}$ . Methods used for the measurement of the activities of  $Ra^{226}$  and  $Po^{210}$  were essentially the same as those previously described (1), with the exception that  $Po^{208}$  was added as a tracer to correct for the radiochemical yield of  $Po^{210}$ .

Eight well-developed plants (*Nicotiana tabacum* L. cv. Catterton, about 45.72 cm tall) were transplanted from the field to buckets 35.56 cm in diameter and 40.61 cm deep and were placed inside a small, closed greenhouse